Analyst

Accepted Manuscript

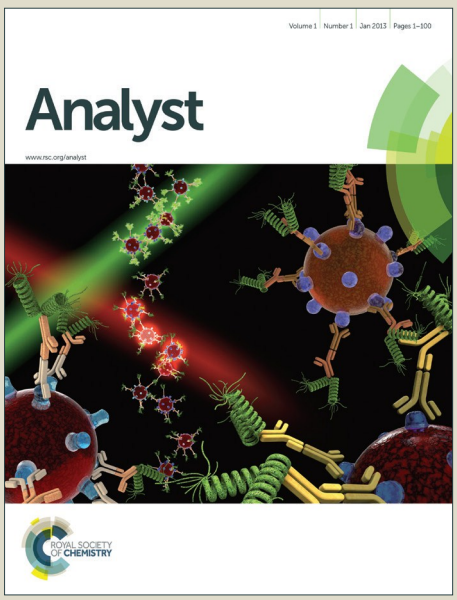

ROYAL SOCIETY OF CHEMISTRY

www.rsc.org/analyst

Analyst

Dynamic Article Links ►

Cite this: DOI: 10.1039/c0xx00000x

www.rsc.org/xxxxxx

ARTICLE TYPE

Aptamer-based colorimetric biosensing of abrin using catalytic gold nanoparticles †

Jingting Hu, [ab] Pengjuan Ni, [ab] Haichao Dai, [ab] Yujing Sun, [a] Yilin Wang, [ab] Shu Jiang, [ab] and Zhuang Li*[a]

Received (in XXX, XXX) Xth XXXXXXXXX 20XX, Accepted Xth XXXXXXXXX 20XX

DOI: 10.1039/b000000x

In this study we propose a simple and sensitive colorimetric aptasensor for the quantitative analysis of abrin by using catalytic AuNPs for the first time. AuNPs possess the peroxidase-like activity that can catalyse 3, 3, 5, 5-tetramethylbenzidine (TMB) in the presence of H_2O_2 , leading to color change of the solution. It is interesting to find that the peroxidase-like activity of AuNPs can be improved by surface activation with target-specific aptamer. However, with target molecule, the aptamer is desorbed from the AuNPs surface, resulting in a decrease of the catalytic abilities of AuNPs. The color change of the solution is relevant to the target concentration, and this can be judged by the naked eye and monitored by UV-vis spectrometer. The linear range for the current analytical system was from 0.2 nM to 17.5 nM. The corresponding limit of detection (LOD) was 0.05 nM. Some other proteins such as thrombin (Th), glucose oxidase (GOx), and bovine albumin (BSA) all had a negligible effect on the determination of abrin. Furthermore, several practical samples spiked with abrin were analyzed using the proposed method with excellent recoveries. This aptamer-based colorimetric biosensor is superior to the other conventional methods owing to its simplicity, low cost, high sensitivity.

1.Introduction

Abrin is a highly toxic protein which is found in the beans of *Abrusprecatorius*. Along with ricin, it belongs to the type II ribosome inactivating protein family [1]. Abrin has been found to be more toxic than its counterpart ricin, with a human lethal dose of 0.1–1 μg/kg [2] as compared to 5–10 μg/kg for ricin inhalation [3]. The abrin toxin consists of two non-identical polypeptide chains (A and B) cross linked by a single disulfide bond. The A-chain is an efficient N-glycosidase and is transported across the plasma membrane by the B-chain via endocytosis into the cytoplasma of cells. Once internalized, the A-chain removed an adenine from an exposed loop of 28s ribosomal RNA, thus inhibiting protein synthesis and resulting in eventual cell death [4-7]. Abrin should be closely monitored as a threatening biological agent due to its easy cultivation and cheap preparation, and it is included in the Biological and Toxin Weapons Convention (BTWC) Procedural Report (2001) [8]. Hence, the researches focused on rapid detection and specific recognition of abrin toxin should be paid more attention.

Several technologies have been developed for abrin detection, including surface-enhanced Raman spectroscopy [9], Electrochemiluminescent assay [10], liquid chromatography tandem mass spectrometry (LC/MS) [11], and antibody-based immunoassays [12, 13]. Although, these assays are effective for abrin detection, most of these analytical methods rely on sophisticated instruments and skilled manpower, making such approaches impractical for on-site detection.

Of the alternatives to antibody-based sensing assays, aptamer-based methods have become popular over the past decades due to their inherent selectivity, affinity, and multifarious advantages over the traditional recognition elements. As a new class of single-stranded DNA/RNA molecules, aptamers are selected in vitro by the systematic evolution of the ligand by the exponential enrichment (SELEX) process from random-sequence nucleic acid libraries. These molecular ligands have the ability to recognize their cognate targets with high affinity and specificity. This property makes aptamers an ideal tool to detect a variety of target molecules including proteins, drugs, small molecules, inorganic ions and even cells.[14-19]

Nowadays, increasing attention has been paid to the nanoscaled peroxidase mimetics and their potential applications in bioanalysis [20-26] since the first Fe_3O_4 magnetic nanoparticles-based peroxidase was reported [27]. A variety of nanomaterials have been also demonstrated to possess intrinsic peroxidase-like activity. Although gold is usually viewed as an inert metal, surprisingly it has been found that AuNPs possess intrinsic peroxidaselike activity.[28, 29] The findings show that a catalytic

[a] *State Key laboratory of Electroanalytical Chemistry, Changchun Institute of Applied Chemistry, Chinese Academy of Sciences, Changchun, Jilin 130022, PR China*

[b] *University of Chinese Academy of Sciences, Beijing, 100039, PR China*

Fax: +86 431 85262057; Tel: +86 431 85262057; E-mail: zli@ciac.jl.cn

† Electronic Supplementary Information (ESI) available:. See DOI: 10.1039/b000000x/

AuNP-based strategy has enormous potentials in detection and can be exploited to develop biosensors for a wide variety of target analytes.

Enlightened by the above facts, we propose an aptamer-based colorimetric biosensor of abrin based on the peroxidase-like activity of gold nanoparticles. Abrin binding aptamer (ABA) can be absorbed onto the surface of AuNPs and improve the ability of AuNPs to catalyze 3, 3, 5, 5-tetramethylbenzidine (TMB) in the presence of H_2O_2 and lead to the significant enhancement of the absorbance. However, in the presence of abrin, the ABA undergoes target-responsive structural changes followed by desorption from the AuNPs surface to allow an aptamer-target binding event, resulting in a decrease in the catalytic abilities of AuNPs. The high selective and sensitive detection of abrin is possible using the naked eye or monitored by UV-vis spectrometer. Furthermore, the proposed method does not require any modification of the aptamer, making it time-saving and cost-effective.

2. Experimental

2.1. Reagent and chemicals

Abrin was purchased from Beijing Hapten and Protein Biomedical Institute (Beijing, china). The sequence of abrin binding aptamer (ABA) was 5'-ATCCTGTGAGGAATGCTCATGCATAGCAAGGGCT-3'. [30] The ssDNA oligonucleotides were synthesized by Shanghai Sangon Biotechnology Co. Ltd. (Shanghai, China) and the lyophilized powder was dissolved in distilled water and before use it was stored at 4 ℃. The concentration of the oligonucleotide was determined by measuring the UV absorbance at 260 nm. Chloroauric acid ($HAuCl_4$•$4H_2O$) was obtained from Shanghai Chemical Reagent Company (Shanghai, China). 3, 3, 5, 5-tetramethylbenzidine (TMB) and Hexadecyl trimethyl ammonium Bromide (CTAB) was purchased from Aladdin Reagent Company (Shanghai, China). Thrombin (Th), glucose oxidase (Gox), and bovine albumin (BSA) were purchased from Sigma-Aldrich Chemical Co (Milwaukee, WI, USA). $C_6H_5Na_3O_7$, H_2O_2, Na_2HPO_4·$12H_2O$ and NaH_2PO_4 $2H_2O$ were obtained from Beijing Chemical Reagent Company. All of the reagents were analytic grade and used as received. Ultrapure water obtained from a Millipore water purification system (≥18 MΩ, Milli-Q, Millipore) was used in all runs.

2.2. Instrumentation

The ultraviolet-visible (UV-vis) absorption spectra were recorded on a Cary 50 Scan UV-vis spectrophotometer (Varian, USA) at 25℃. The zeta potentials were measured on Malvern Zetasizer Nanoseries at 25 ℃. Transmission electron microscopy (TEM) measurements were made on a Hitachi H-8100 transmission electron microscope operated at an accelerating voltage of 100 kV.

2.3. Synthesis of the citrate-protected AuNPs

AuNPs were synthesized using the classical citrate reduction method.[31] Briefly, colloidal AuNPs with an average diameter of 13 nm were prepared by rapidly injecting a sodium citrate solution (10 mL, 38.8 mM) into a boiling aqueous solution of $HAuCl_4$•$4H_2O$ (100 mL, 1 mM) with vigorous stirring. After boiling for 30 min, the reaction flask was removed from the heat to allow the reaction solution to cool at room temperature. The concentration of the AuNPs was about 10 nM, which was determined according to Beer's law by using the extinction coefficient of $2.78*10^8\ M^{-1}\ cm^{-1}$ for 13 nm AuNPs in diameter at 520 nm. [32]

2.4. Detection of abrin using colorimetric biosensing method

A typical colorimetric analysis was realized as following procedure: first, 100 μL of 2.5 nM 13 nm AuNPs was mixed with 20 μL of 5 μM ABA. Second, 50 μL abrin with appropriate concentration in PB (pH 7.4) was added to the AuNPs/ABA solution. The solutions were allowed to react for 5 min and then 15 μL of 10 mM TMB and 15 μL of 10 M H_2O_2 were added to produce color change. After the solution was equilibrated for 10 min at 25 ℃, and then was transferred to a quartz cuvette. The UV–vis absorption spectra were measured over the wavelength ranging from 550 nm to 750 nm.

2.5. Treatment of raw milk

Milk samples were prepared following a previous method with a minor modification [33]. Briefly, 5.0 mL of raw milk was placed in a 7 mL centrifuge tube, and 1.5 mL of 2 M trichloroacetic acid was introduced. After ultrasonication for 10 min, the mixture was centrifuged at 10,000 rpm for 10 min.

3. Results and discussion

3.1. The mechanism of the sensing system

Recently, it has been demonstrated that the peroxidase-like activity of nanoparticles varied with respect to electrostatic affinity between nanoparticles and substrates. Two substrates that would be helpful to evaluate this point of view.[34, 35] ABTS （negatively charged）possesses two sulfonic acid groups, exhibiting higher affinity toward a positively charged nanoparticle surface. With ABTS as the substrate, cationic nanoparticles displayed a high affinity and subsequently a high peroxidase activity. Conversely, TMB （positively charged）carries two amine groups, exhibiting stronger affinity toward a negatively charged nanoparticle surface. With TMB as a substrate, anionic nanoparticles had a high affinity and exhibited a high catalytic activity.

As mentioned above, Fig. 1 outlines the concept of the catalysis-based colorimetric assay. According to previously reported,[36, 37] a random coil ssDNA (ABA herein) could uncoil sufficiently to expose its bases, which could be easily adsorbed onto the surface of AuNPs. Thus, DNA phosphate backbone with a large number of negative charges existed on the surface of AuNPs. Therefore, with positively charged TMB as a substrate, ABA-AuNPs complex had a high affinity and exhibited a significant enhancement of catalytic activity. However, upon the addition of abrin, ABA bound to abrin followed by desorption from the AuNPs surface and the conformation of ABA was changed from random coil structure to G-quardruplex structure (rigid structure). The rigid structure prevented the exposure of the ABA bases to AuNPs and the negative charges existed on the surface of AuNPs was less, resulting in a decrease of the catalytic abilities of AuNPs.

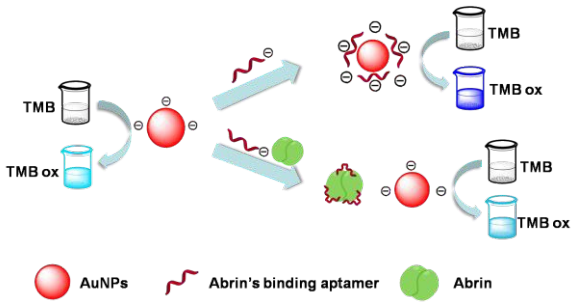

Fig. 1 The mechanism of the aptamer-based colorimetric biosensor for abrin.

3.2. Spectral characteristics

To confirm the feasibility of our concept, the spectral responses of the aptamer-based colorimetric biosensor were observed under different conditions (Fig. 2A). The spectral value of AuNPs alone in solution at 650 nm was 0.8 absorbance units (a.u.) (1, Fig. 2A), explained by the oxidation of colorless TMB to blue TMB ox by catalysis. In the presence of ABA, this value (2, Fig. 2A) increased to 1.25 a.u., indicating the enhancement of catalysis of AuNPs. When abrin molecules were present in the solution (3, Fig. 2A), ABA bound to abrin followed by desorption from the AuNPs, resulting in a decrease of the catalytic abilities of AuNPs. As expected, the addition of abrin alone did not cause the color change of the solution (4, Fig. 2A) compared with AuNPs alone (1, Fig. 2A). Further, the spectral value of AuNPs in the presence of CTAB (a kind of cationic surfactants) at 650 nm was 0.3 (5, Fig. 2A). These results confirm that the negatively charged aptamer is the main cause of the enhancement of AuNP-dependent catalysis. Table 1 shows the Zeta potential of AuNPs under different conditions and the results have agreement with our mechanism.

In order to get rid of the possible impact of oxidation of TMB caused by ABA, abrin, and the abrin-ABA complex, these three molecules were also employed to the oxidation of TMB (Fig. S1). The results indicate that ABA, abrin, and the abrin-ABA complex do not posses the peroxidase-like activity. Fig. S2 shows the morphology characteristics of AuNPs under different conditions. The AuNPs are monodisperse and spherical with the average size of 13 nm (Fig. S2). The UV-visible spectra of AuNPs, AuNPs-ABA, AuNPs-abrin and AuNPs-ABA-abrin complex show a typical Au NPs SPR peaks with maxima at 520 nm, confirming the stability of AuNPs on different conditions (Fig. S3). The observation showed that there was no aggregation of AuNPs caused by ABA, abrin and ABA-abrin complex.

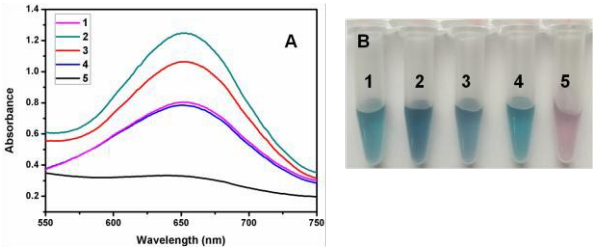

Fig. 2 (A) UV-vis spectra in the presence of TMB and H_2O_2 under different conditions of (1) 1.3 nM AuNPs, (2) 1.3 nM AuNPs + 0. 5 μM ABA, (3) 1.3 nM AuNPs + 0. 5 μM ABA +1 nM abrin, (4) 1.3 nM AuNPs +1 nM abrin, (5) 1.3 nM AuNPs + 0.3 g/L CTAB. (B) The corresponding digital images.

Table 1 Zeta potential of AuNPs under different conditions.

Sample	Zeta potential (mV)
AuNPs[a]	-8.58
AuNPs[a] + ABA[b]	-16.00
AuNPs[a] + ABA[b] + Abrin[c]	-11.10
AuNPs[a] + CTAB[d]	1.03

[a] C_{AuNPs} = 1.3 nM, [b] C_{ABA} = 0.5 μM, [c] C_{Abrin} = 1 nM, [d] C_{CTAB} = 0.3 g/L

3.3. Optimization of the key parameters

The peroxidase-like activity of AuNPs depends on some key parameters, such as the concentration of ABA, TMB and H_2O_2, reaction time, temperature, pH value and the size of AuNPs. Therefore, these key parameters were optimized prior to the application of our proposed method. We used the reduction of absorbance, that is, A_0 - A (ΔA) as a criterion to optimize the detection conditions. A_0 presents the absorbance at 650 nm in the absence of abrin. A presents the absorbance at 650 nm in the presence of 5 nM abrin.

3.3.1. Effect of reaction time

Fig. S4 shows the effect of reaction time on the peroxidase-like activity of the sensing system. It is shown that the ΔA reach a platform from 10 to 20 min. Accordingly, 10 min was chosen as the reaction time. (ESI, Fig. S4†)

3.3.2. Effect of reaction temperature

Temperature is another crucial factor for most enzyme-based system. Fig. S5 shows that the ΔA increase with increasing temperature in the range from 15 ℃ to 25 ℃. Further increase in temperature result in the decrease of ΔA., Therefore, 25 ℃ was chosen as the reaction temperature. (ESI, Fig. S5†)

3.3.3. Effect of ABA concentration

Fig. S6 displays the effect of ABA concentration of the sensing system. It is clear seen from Fig. S5, the concentration of ABA being too high or too low is not suitable for improving the sensitivity. The ΔA is reduced with increasing ABA concentration in the range from 0.5 μM to 0.7 μM and this fits to the theory that abrin compete with AuNPs for binding to ABA and the least surface activated AuNPs amount of ABA means the most sensitivity. However, 0.2, 0.3, 0.4 μM ABA is too small to improve the peroxidase-like activity of AuNPs. Hence, the concentration of ABA was selected to be 0.5 μM for this experiment. (ESI, Fig. S6†)

3.3.4. Effect of H_2O_2 and TMB concentration

The impact of TMB and H_2O_2 concentration on the sensitivity of sensing system was examined. Fig. S7 shows that ΔA increased with increasing H_2O_2 concentration from 0.3 M to 0.75 M and

then it reduces with increasing H_2O_2 concentration in the range from 0.75 M to 1 M. Fig. S8 shows that ΔA increased with increasing TMB concentration from 0.3 mM to 0.75 mM and then it reduces with increasing TMB concentration in the range from 0.75 mM to 1 mM. These results suggest that the reaction of H_2O_2 with TMB catalyzed by AuNPs reached equilibrium when the concentration of H_2O_2 and TMB were 0.75 M and 0.75 mM. Therefore, 0.75 M of H_2O_2 and 0.75 mM of TMB was chosen for the next experiments. (ESI, Fig. S7, Fig. S8†)

3.3.5. Effect of pH value

pH is an crucial factor for almost every sensing system. Fig. S9 displays the effect of pH value of the sensing system. It is shown that ΔA increase with increasing pH value in the range from 6.2 to 7.4. Further increase of pH value results in the decrease of ΔA. Therefore, pH 7.4 was adopted in the following experiments. (ESI, Fig. S9†)

3.3.6. Effect of the size of AuNPs

Fig. S10 shows the morphology characteristics of AuNPs with different sizes (13 nm, 25 nm and 40 nm) and Fig. S11 shows the effect of AuNPs size of the sensing system. The results show that the ΔA for 13 nm, 25 nm and 40 nm AuNPs solution is 0.292, 0.212, 0.182, respectively, under the similar experimental condition. Thus, we used 13 nm AuNPs as the following experiment condition on basis of higher sensitivity. (ESI, Fig. S10, Fig. S11†)

3.4. Colorimetric biosensing of abrin

Under the optimal detection conditions, the peroxidase-like of the AuNPs on TMB oxidation in the presence of various concentration of abrin was investigated. The ΔA at 650 nm in the presence of different amounts of abrin are shown in Fig. 3A. The digital images shows that with increasing abrin concentration, the color of the solution changed from dark blue to light blue, suggestive of the abrin concentration-dependent TMB catalysis. It can be evidently observed that the ΔA at 650 nm increase gradually with the increasing concentration of abrin. In another word, with the increasing concentration of abrin, the peroxidase-like activities of AuNPs decreased. This observation is accord with our hypothesis. As shown in Fig. 3B, the ΔA exhibits a good linear relationship with logC (abrin, nM) in the concentration range from 0.2 nM to 17.5 nM (R^2=0.995). The detection limit can reach as low as 0.05 nM at a signal-to noise ratio of 3, which is lower than many previous reports. In addition, we compared the detection limit and detection time of the reported method. **Table 2** shows the comparison of different methods for abrin detection. The analytical parameters are comparable or even better than those reported in the literature. The previous methods suffer from some disadvantages. SERS assay [9], electrochemiluminescent assay [10] and LC/MS assay [11] rely on sophisticated instruments. Enzyme linked immunosorbent assay [12, 13] requires a specific antibody against the analyte, which demands high cost and time consuming work. Aptamer-based fluorescent biosensor strategy [30] need aptamer to be labeled with signal materials and the introduction of a labeling substance makes the assay more complicated, time consuming and laborious. While our aptamer-based colorimetric biosensor assay only need cheap instrument and simple design, and can be performed without the presence of trained technician. In addition, our strategies did not need aptamer to be labeled with signal materials. Thus makes the assay with the advantages of convenience, low cost, time saving and ease of operation.

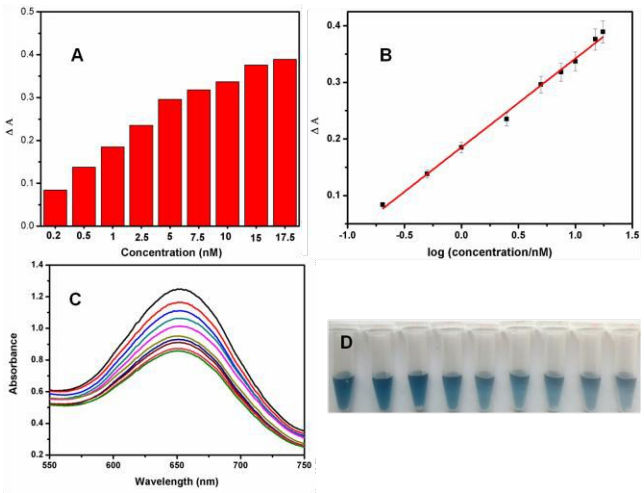

Fig. 3 (A) ΔA at 650 nm in the presence of various concentration of abrin. (B) Typical calibration curve for abrin obtained using the aptamer-based colorimetric biosensor. （C）Uv-vis spectra in the presence of various concentration of abrin (0 nM, 0.2 nM, 0.5 nM, 1 nM, 2.5 nM, 5 nM, 7.5 nM, 10 nM, 15 nM, 17.5 nM)（D） The corresponding digital images.

Table 2 Comparison of different method for abrin detection

Detection method	Detection limit	Detection time (including pre-treatment time)
SERS assay [9]	0.1 ng mL^{-1}	11.5 h
Electrochemiluminescent Assay [10]	0.5 ng mL^{-1}	17 h
Enzyme linked immunosorbent assay [12]	7.8 ng mL^{-1}	15 h
LC/MS assay [11]	25 ng mL^{-1}	Not given
Enzyme linked immunosorbent assay [13]	35 ng mL^{-1}	15 h
Aptamer-based fluorescent biosensor assay [30]	60.8 ng mL^{-1}	Not given
Aptamer-based colorimetric biosensor assay (this work)	0.05 nM (2.5 ng mL^{-1})	1h

3.5. Selectivity

The developed aptamer-based colorimetric biosensor is also specific. To evaluate this property, we challenged the system with the target abrin (5 nM) and several nontargeted proteins such as Thrombin (Th), glucose oxidase (Gox), and bovine albumin (BSA) (all at such as 5 nM). Fig. 4 shows that ΔA at 650 nm in the presence of abrin is considerably larger than those of other proteins. The results indicate that our approach has a high specificity to abrin.

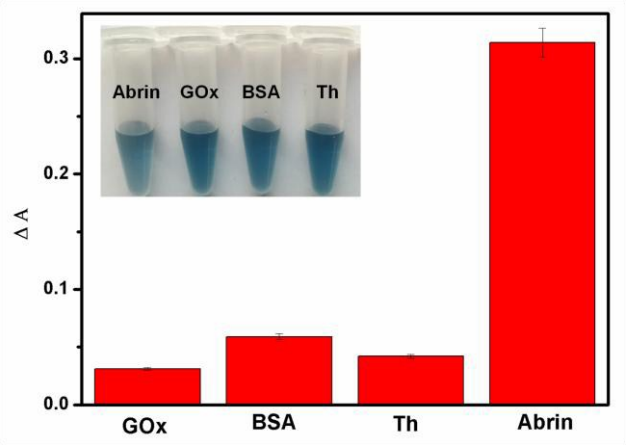

Fig. 4 The selectivity of the proposed system towards abrin detection. The concentration of abrin and other proteins are 5 nM. Inset shows the corresponding digital images.

3.6. Application in practical samples

In order to evaluate the feasibility of the present method in practical applications, the detection of abrin in raw milk was carried out. The practical samples were spiked with certain amounts of abrin. **Table 3** shows that the recoveries of the practical samples are in the range 96.5% to 110.0%. The desirable recoveries demonstrate the reliability of the proposed method for detection of abrin in practical applications.

Table 3 Analytical results for abrin in raw milk samples.

Sample	Add (nM)	Found (nM) [a]	Recovery (%)	RSD (%)
Raw milk 1	3.0	3.3 ±0.04	110.0	1.36
Raw milk 2	17.5	16.9 ±0.2	96.5	1.18

[a]Average of three determinations ±standard deviation

Conclusions

In summary, we have successfully developed a sensitive, accurate and reliable aptamer-based colorimetric biosensor for the determination of abrin based on peroxidase-like activity of gold nanoparticles without complicated modification and expensive instruments. The dark-blue to light-blue color change in the presence of abrin was found to be easily observed by the naked eye or measured by UV-vis spectrometer. The linear range and its detection limit were found to be 0.2 nM to 17.5 nM and 0.05 nM, respectively. More importantly, the proposed method is successfully applied to the detection of abrin in practical samples. Therefore, this method may offer a new approach for developing simple, low cost and sensitive sensors for abrin detection.

Acknowledgment

Financial support by the National Basic Research Program of China (973 program, no. 2010CB933600), the National Natural Science Foundation of China (21275135 and 21405146) is gratefully acknowledged.

References

1. J. Cheng, T.H. Lu, C.L. Liu, J.Y. Lin. J. *Biomed. Sci.*, 2010, 17, 34.
2. K. Dickers, K. Bradberry, P. Rice, G. Griffiths, J.A. Vale, *Toxicol. Rev*., 2003, 22, 137–142.
3. S. Bradberry, K. Dickers, P. Rice, P. Griffiths, J.A. Vale, *Toxicol. Rev*., 2003, 22, 65–70.
4. S. Olsnes, K. Refsnes, A. Pihl, *Nature*, 1974, 249, 627.
5. Y. Endo, K. Mitsui, M. Motizuki, K. Tsurugi, *J. Biol.Chem*., 1987, 262, 5908.
6. G.D. Griffiths, M.D. Leek, D.J. Gee. *J. Pathol*, 1987, 151, 221.
7. J.N. Hughes, C.D. Lindsay, G.D. Lindsay, *Hum. Exp. Toxicol*., 1996, 15, 443.
8. X.B. Li, W. Yang, Y. Zhang, Z.G. Zhang, T. Kong, D.N. Li, J.J. Tang, L. Liu, G.W. Liu, Z. Wang, *J. Agric. Food Chem*., 2011, 59, 9796–9799.
9. H. Yang, M. Deng, S. Ga, S. H. Chen, L. Kang, J. H. Wang, W. W. Xin, T. Zhang, Z. R. You, Y. An, J. L. Wang, D.X. Cui, *Nanoscale Res. Lett*., 2014. 9:138
10. E. A. E. Garber, J. L. Walker, T. W. O'Brien, *J. Food Prot.*, 2008, 71, 1868–1874
11. J. Owens and C. Koester, *J. Agric. Food Chem.*, 2008, 56, 11139–11143.
12. X. B. Li, W. Yang, Y. Zhang, Z. G. Zhang, T. Kong, D. N. Li, J. J. Tang, L. Liu, G. W. Liu, Z. Wang, *J. Agric. Food Chem.*, 2011, 59, 9796 – 9799.
13. H. Y. Zhou, B. Zhou, H. Z. Ma, C. Carney, K. D. Janda. Bioorg, *Med. Chem. Lett.*, 2007, 17, 5690-5692.
14. A. D. Ellington and J. W. Szostak, *Nature*, 1990, 346, 818–822.
15. T. Kunii, S. Ogura, M. Mie and E. Kobatake, *Analyst*, 2011, 136, 1310–1312.
16. J. Lee, M. Jo, T. H. Kim, J. Y. Ahn, D. K. Lee, S. Kim and S. Hong, *Lab Chip*, 2011, 11, 52–56.
17. R. L. Srinivas, S. C. Chapin and P. S. Doyle, *Anal. Chem*., 2011, 83, 9138–9145.
18. C. Tuerk and L. Gold, *Science*, 1990, 249, 505.
19. W. Yuanboonlim, W. Siripornnoppakhun, N. Niamnont, P. Rashatasakhon, T. Vilaivan and M. Sukwattanasinitt, *Biosens. Bioelectron*., 2012, 33, 17–22.
20. Y. Jv, B. Li, R. Cao, *Chem. Commun.*, 2010. 46 (42), 8017–8019.
21. S. Wang, W. Chen, A. Liu, L. Hong, H. Deng and X. Lin, *ChemPhysChem*., 2012. 13 (5), 1199–1204.
22. Z. Gao, M. Xu, L. Hou, G. Chen and D. Tang, *Anal. Chim. Acta*, 2013. 776, 79–86.
23. H. Jiang, Z. Chen, H. Cao and Y. Huang, *Analyst*, 2012.137 (23), 5560–5564.
24. X. Wang, Q. Wu, Z. Shan and Q. Huang, *Biosens. Bioelectron.*, 2011. 26 (8), 3614–3619.
25. J. Tian, Q. Liu, A. Asiri, A. Qusti, A. Al-Youbi and X. Sun, *Nanoscale*, 2013. 5 (23), 11604–11609.
26. Q. Chen, M.L. Liu, J.N. Zhao, X. Peng, X.J. Chen, N.X. Mi, B.D. Yin, H.T. Li, Y.Y. Zhang and S.Z. Yao, *Chem. Commun*., 2014. (50), 6771-6774.
27. L. Gao, J. Gao, L. Nie, J. Zhang, Y. Zhang, N. Zhang, T. Wang, J. Wang, D. Wang, S. Perrett, and X. Yan, *Nat. Nanotechnol*., 2007, 2 (9), 577 – 583.
28. M. Comotti, C. Della Pina, R. Matarrese and M. Rossi, *Angew. Chem., Int. Ed*., 2004, 43, 5812;
29. Y. Lin, Z. Li, Z. Chen, J. Ren and X. Qu, *Biomaterials*, 2013, 34, 2600.
30. J. J. Tang, T. Yu, L. Guo, J. W. Xie, N. S. Shao, Z. K. He, *Biosens. Bioelectron*., 2007, 22, 2456–2463
31. G. N. Mayer, *Nucleic Acid and Peptide Aptamers: Method and Protocols*. Humana, New York, NY, 2009.
32. M. M. Maye, L. Han, N. N. Kariuki, N. K. Ly, W. B. Chan,J. Luo and C.-J. Zhong, *Anal. Chim. Acta*, 2003, 496, 17 – 27.
33. X. F. Li, J. Li, H. Y. Kuang, L. Feng, S. J. Yi, X. D. Xia, H. W. Huang, Y. Chen, C. R. Tang and Y. L. Zeng, *Anal.Chim. Acta*, 2013, 802, 82 – 88.
34. F. Yu, Y. Huang, A.J. Cole and V.C. Yang, *Biomaterials*, 2009, 30, 4716–4722.
35. Y.P. Liu and F.Q. Yu, *Nanotechnology*, 2011, 22, 145704.
36. H. X. Li and L. J. Rothberg, Anal. Chem., 2004a, 76(18), 5414–5417
37. H. X. Li and L. J. Rothberg, J. Am. Chem. Soc., 2004b, 126(35),10958–10961.

A facile colorimetric aptasensor for abrin based on the peroxidase-like activity of gold nanoparticles was demonatrated for the first time.